ARCHIVE EDITION OF

IRPS BULLETIN

Volume 21 No 1 March, 2007

Office Bearers : 2006 - 2009

Cover of this Journal

Editorial

President's Column

The Bouguer-Lambert-Beer Absorption Law

Members' Paper

Return to Archive Home Page

COVER OF VOLUME 21 NO. 1, March 2007

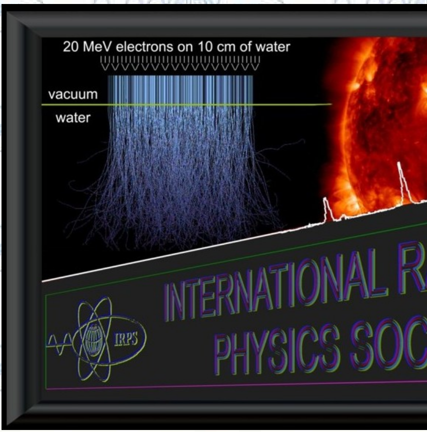
20 MeV electrons on 10 cm of water
vacuum
water
IRPS
INTERNATIONAL R
PHYSICS SOC

> "The important thing is not to stop questioning.
> Curiosity has its own reason for existing.
> One cannot help but be in awe when he contemplates
> the mysteries of eternity, of life, of the marvelous
> structure of reality.
> It is enough if one tries merely to comprehend
> a little of this mystery every day."
>
> * Albert Einstein *

Home Page | Next

EDITORIAL

Welcome to the first issue of Volume 21 of the IRPS Bulletin. In addition to Society news and business, we continue to invite technical content of interest to our radiation-physics community. In this issue, long-standing member Leif Gerward presents an unattenuated review of the Absorption Law and the historical figures who did "not stop questioning" as the Einstein quote urges on the cover page. This is appropriately followed by a member paper on absorption coefficients which itself references the fundamental work of Gerward.

At a time when the world news headlines are filled with discord, the members of the International Radiation Physics Society can take pride in uniting across boundaries of space and ideology to promote and disseminate the fruits of our collected work. As our President points out in his column, there are dimensions of this work that intersect with global and societal issues and we are in the best position to offer unbiased guidance on their technical aspects. Some will suggest that consensus is impossible because we are too often blinded by agendas of self interest. Maybe so, but are we willing to make the attempt?

Please be encouraged to submit comments or position papers on what our President has called the 'radiation debates' that are constructive and informed by the multidimensional aspects of these global problems. We may also publish letters to the editor that comment in turn on these position papers. It is hoped that the unity of purpose that makes us a society is not threatened by such a discussion, but rather that such discussion will add meaning to that purpose.

Larry Hudson

Home Page | Next

PRESIDENT'S REPORT

I regret to inform you that John Hubbell, one of the founding fathers of our society died in hospital on 31 March 2007, John suffered a massive stroke in late February, resulting in paralysis to his right side and loss of speech. He recovered sufficiently to be moved to a convalescent unit, but a subsequent episode and pneumonia saw him returned to hospital where he finally succumbed to his illness. An obituary will be included in the next issue of the IRPS Bulletin.

We all shall miss him.

Many members of the IRPS are indebted to John for assistance in many ways. For almost fifty years, John acted as the "clearing house" for all information on the scattering of "hard radiation": radiation in the energy range from soft X-rays to cosmic radiation. Over this period, there were many instances where governments were in disputation with one another, or were restrictive in their interactions. Nevertheless, John continued to provide information, encouragement, advice, and support to scientists of all nationalities with true generosity of spirit.

The IRPS tries to carry on this work. It is our aim to provide encouragement and support for scientists of all nations, with the stronger nations assisting the weaker. We hold our symposia and workshops with the aim of bringing knowledge and awareness in the broad spectrum of radiation physics to as many scientists from as many nations as we can. And we try to provide financial support for those from developing countries to attend these meetings.

But perhaps we should become more involved in the "radiation debates" which are occurring in our separate communities. We live in a time where the internet and television disseminate "information" to the international community. Much of this "information" is misleading, or downright incorrect. The use of un-provenanced and untested information by journalists, politicians, and self-interest groups brings with it the likelihood that incorrect decisions on issues crucial to the environmental health of our global community will be made: to everybody's detriment.

"Climate change" is one of these global issues. Personally, I am concerned that in discussions on climate change, issues, such as whether nuclear power should be in the mix of alternative sources to be used, are treated by the media in only the most simplistic fashion. The same statement applies to the subject of the use of solar radiation as an energy source. And the issue of radiation safety, whether it be protection against radiation from nuclear waste products or from solar radiation, is seemingly never addressed sensibly in media releases.

There are many other such issues of global concern. And surely it is time to redress the imbalance between incorrect and correct information in the public debate on these crucial matters. A good start may be for members of the IRPS with expertise in these areas to submit articles on these topics to the Editors of this Bulletin for publication. These would then be subjected to peer review prior to publication. Members would then be better informed on critical issues.

Dudley Creagh

Previous | Home Page | Next

The Bouguer-Lambert-Beer Absorption Law

Leif Gerward

Department of Physics, Technical University of Denmark
DK-2800 Lyngby/Denmark

Introduction

It is well known that the intensity I of light (or other electromagnetic radiation) should decrease exponentially with the distance d that it enters an absorbing medium, i.e.

$$I = I_0 \exp(-\mu d) \qquad (1)$$

where I_0 is the intensity of the incident radiation, and μ is the linear absorption (or attenuation) coefficient. ***Equation (1)*** is usually known as Lambert's law of absorption (e.g. Ballentyne and Lovett, 1970). However, there is some confusion about the origin of that law, since other names are Lambert–Beer's law and Bouguer's law. Therefore, it should be interesting to know a little more about the scientists associated with the Absorption Law, and about their contributions to the subject.

As it turns out, the story has already been told. Fred Perrin (1948) has published a note with the somewhat provocative title "Whose Absorption Law?" Perrin's paper, however, appeared almost sixty years ago, and few may be aware of it today. Thus, for the benefit of the reader of the Bulletin, it should be worthwhile once again to discuss the origin of the Absorption Law. I have also extended the scope of the present paper by including biographical sketches of Bouguer, Lambert and Beer.

Pierre Bouguer (1698–1758)

Pierre Bouguer was a child prodigy trained by his father, Jean Bouguer, who was a professor of hydrography at Croisic in Lower Brittany, France. The father died when Pierre was 15 years old, but by then the son had already acquired enough knowledge in mathematics and natural sciences to succeed in the chair of his father. In spite of his young age, Pierre lectured with great authority on topics such as mathematics, physics and astronomy. The French ***Académie des Sciences*** awarded him several prizes for his work, and in 1731 he became himself a member of the Academy. In 1735 he participated in an expedition to Peru to measure the length of a degree of meridian at the equator (this expedition was part of a larger project aimed at determining the shape of the Earth). Bouguer also measured gravity at different altitudes and was the first to estimate the gravitational pull of mountains, the so-called Bouguer correction.

Pierre Bouguer ***(Fig. 1)*** devoted most of his professional life to the solving of nautical problems. However, he is also known as the father of photometry. In 1729 he published an extensive work, ***Essai d'optique sur la gradation de la lumière***, where he laid the foundation of this branch of science. In the present context it is interesting to note that Bouguer, among other things, investigated the absorption of light in the atmosphere and other transparent media. Bouguer's optical work was posthumously published in 1760 as ***Traité d'optique sur la gradation de la lumière***.

Chapter two of the ***Essai d'optique*** deals with transparency and opacity of matter. Bouguer takes the trouble to explain in detail how the intensity of light decreases upon traversing a transparent body. In his model, the body is divided into a number of layers of equal thickness, and the light rays are incident perpendicular to the layers. At first sight, one might think that the intensity of light should decrease in arithmetical progression, but Bouguer argues that this cannot be true. Instead, as he correctly points out, the intensity will always decrease in geometrical progression, since each layer absorbs a constant fraction of the intensity incident upon it. Therefore,

> the intensity of light, after traversing different thicknesses, can be represented by the ordinates of a logarithmic [curve], which has the thickness of the medium as its axis [of abscissae] (Bouguer, 1729).

As noticed by Bouguer, the logarithmic curve, which is well known to mathematicians and surveyors, has the properties that the subtangent is constant and, most importantly in the present case, the ordinates decrease in geometrical progression.

In order to illustrate his point, Bouguer considers a perfectly homogenous body ABCD, divided into layers of equal thickness ***(Fig. 2).*** The light is incident perpendicular to the face AB. The length QB represents the incident intensity. After having traversed the depth BF or AE, the light enters the second layer through the face EF. At this depth the intensity is RF. In this way, the intensity as a function of depth can be described by the logarithmic curve QRXY, where BC is the axis of abscissae (the ***x***-axis). For a less transparent body the intensity will decrease more rapidly. In fact, the shape of the transmission curve is determined solely by its subtangent and by the intensity of the incident radiation. Bouguer then goes on, giving several examples of how transmission curves can be constructed and used in various problems.

It follows from above that Bouguer has given a correct description and interpretation of the transmission of light in a transparent body, although he has not expressed the Absorption Law in the concise form of ***Equation (1),*** later to be derived by Lambert.

Johann Heinrich Lambert (1728–1777)

Johann Heinrich Lambert was an autodidact, who had to rely on his own efforts for his education. Son of a poor tailor in Mühlhausen, Elsass (Alsace), he had to leave school at the age of twelve to help his father with tailoring. At the age of fifteen he worked as a clerk at the nearby ironworks to earn money for the family. Two years later, he took up a position as secretary to Professor Iselin, the editor of a newspaper at Basel, Switzerland. Lambert could now use his spare time for studies in natural sciences and philosophy.

In 1748, Iselin recommended the young Lambert for a position as private tutor in the home of Count Peter von Salis, who lived in Chur, Switzerland. Here, Lambert got access to the excellent library of the Count, and he seized the opportunity to delve deeply into mathematics, astronomy and philosophy. While in Chur, Lambert first came to be noticed by the scientific community of his time. He made his own astronomical instruments, and he began to publish articles in scientific journals. In 1756 Lambert left Chur with two of the older boys he had tutored during the previous eight years. Lambert and the two young men made a "grand tour" of Europe, of two years duration, visiting several cities and scientific centres, such as Göttingen, Utrecht, Paris, Marseilles and Turin.

Soon after the grand tour, the thirty years old Lambert resigned his tutorship and settled for a while in Augsburg, Germany. Subsequently, Munich, Erlangen, Chur and Leipzig became for brief intervals his home in search for a scientific position. Finally, in 1764, he got a call to join the Berlin Academy of Sciences, founded by Frederick the Great of Prussia. Director of the Berlin Academy was the famous Swiss mathematician Leonhard Euler, who in 1766 was succeeded by the equally famous Italian-French mathematician Joseph Louis Lagrange.

Lambert ***(Fig. 3)*** was a prolific writer. As a member of the Prussian Academy for twelve years, until his death at the age of forty-nine, he produced more than 150 works for publication. He was recognized as one of the best mathematicians of his day. For example, he provided the first rigorous proof that the number pi is irrational, and he made the first systematic development of hyperbolic functions. Lambert made many innovations in the study of heat and light, and several physical laws and units are named after him. In 1760 he published his great work on photometry, ***Photometria sive de mensura et gradibus luminus, colorum et umbrae***. Lambert also made a major contribution to philosophy, and he corresponded with the German philosopher and cosmologist Immanuel Kant.

Lambert successfully found functional equations by expressing physical properties in the language of the differential calculus. Thus, he was first to express Newton's second law of motion in the notation of differential calculus and, most interestingly in the present context, he derived the Absorption Law in the concise form of ***Equation (1)***.

In his ***Photometria***, Lambert derives the Absorption Law in much the same way as can be seen in modern textbooks. He considers a differential layer with thickness dx at distance x into the absorbing body. He then assumes that the fractional reduction of the beam intensity, $-dI/I$, is proportional to the density of the medium and the layer thickness dx, and he arrives at the following differential equation:

$$-dI = \mu I dx \qquad (2)$$

where the linear attenuation coefficient μ is proportional to the density of mass, ρ (modern data tabulations are usually in terms of the mass attenuation coefficient, μ / ρ). For simplicity, I am here using the modern notation, although Lambert uses a slightly different notation in his original paper:

Integrating ***Equation (2)***, one obtains the intensity after traversing the distance d into the absorbing body:

$$\ln(I_0 / I) = \int_0^d \mu \, dx \qquad (3)$$

For a homogenous medium, Eaquation (3) reduces to :

$$\ln(I_0 / I) = \mu \, d \qquad (4)$$

from which the exponential absorption law of ***Equation (1)*** follows.

August Beer (1825–1863)

August Beer appears to have had a smooth career. He was born in Trier, Germany, where he studied mathematics and natural sciences. He continued, working for the mathematician and physicist Julius Plücker (who in 1857 discovered the cathode rays) in Bonn, and obtained his doctorate in 1848. Two years later, he was appointed professor of mathematics and physics at the University of Bonn. In 1854, he published a book on optics, "Einleitung in die höhere Optik".

In 1852, Beer published a paper on the absorption of red light in coloured aqueous solutions of various salts. Beer makes use of the fact, derived from Bouguer's and Lambert's absorption laws, that the intensity of light transmitted through a solution at a given wavelength decreases exponentially with the path length d and the concentration c of the solute (the solvent is considered non-absorbing). Actually, the "Absorption Coëfficient" defined by Beer in his paper is the transmittance (or transmission ratio), $T = I / I_0$. Thus, as pointed out by Beer,

> the transmittance of a concentrated solution can be derived from a measurement of the transmittance of a dilute solution (Beer, 1852).

Indeed, the transmittance measured for any concentration and path length can be normalized to the corresponding transmittance for a standard concentration and path length. Beer in a number of experiments confirms this, defining a standard concentration of 10 %, and a standard path length of 10 cm. The photometer, devised by Beer, is shown in ***Fig. 4***.

Explicitly, Beer's absorption law for a solute in a non-absorbing solvent can be expressed as

$$A = \ln = \left(\frac{I_0}{I}\right)\varepsilon' cd \qquad (5)$$

where A is the absorbance (formerly, and still widely, the optical density) and ε' is the molar absorption coefficient (formerly the extinction coefficient). The molar absorption coefficient ε' is normally expressed in units of L mol^{-1} cm^{-1}. Alternative units are cm^2 mol^{-1}. This change of units emphasizes the point that ε' is a molar cross section for absorption.

In spectroscopy and spectrometry it is common practice to convert the logarithm to base 10. Using the relation $\ln x = \ln 10 \times \log x$, it is easy to show that Beer's law can be expressed as

$$A = \log = \left(\frac{I_0}{I}\right)\varepsilon' cd \qquad (6)$$

where the molar absorption coefficient ε' is given by

$$\varepsilon' = \varepsilon'/\ln 10 = 0.4343\varepsilon' \qquad (7)$$

In passing, it may be mentioned that Beer's law also can be applied to gaseous mixtures, for example the atmosphere. The concentration of each constituent gas is then usually expressed in terms of its partial pressure.

Conclusions

In some sense it is appropriate to name the Absorption Law after Lambert, since he was first to derive ***Equation (1)*** in its concise form using differential calculus. However, one should remember that in principle Bouguer has priority, since he was first to describe the transmission of light in a transparent body in terms of the logarithmic curve. The notation Beer's Law, on the other hand, should be reserved for ***Equations (5)*** and ***(6)***, describing the special case of attenuation of light (or other electromagnetic radiation) in a solution. The present author once remarked that

> if measurements of attenuation coefficients of solutions become common practice, it might be useful to quote the atomic cross sections in units of cm^2/mol instead of the presently accepted units of b/atom or b/molecule (Gerward, 1996).

If so, Lambert's Law and Beer's Law would merge into a single Absorption Law.

Acknowledgment

I wish to thank John H. Hubbell for kindly copying the papers by Bouguer and Lambert from his file.

References

D.W. Ballentyne and D.R. Lovett, ***A Dictionary of Named Effects and Laws in Chemistry, Physics, and Mathematics***, 3rd Ed. Chapman and Hall Ltd., London 1970, p. 188.

A. Beer, Bestimmung der Absorption des rothen Lichts in farbigen Flüssigkeiten. ***Annal. Phys. Chem.*** 86 (1852) 78-88.

P. Bouguer, ***Essai d'optique sur la gradation de la lumière***. Gauthier-Villars et Cie, Paris 1729 (reprinted in 1929 with a Biographic note and a Preface).

L. Gerward, On the attenuation of X-rays and gamma rays in dilute solutions. ***Radiat. Phys. Chem.*** 48 (1996) 697-699.

J.H. Lambert, ***Photometria sive de mensura et gradibus luminus, colorum et umbrae*** (1760). Published in German by E. Anding under the title ***Lambert's Photometrie***, Verlag von Wilhelm Engelmann, Leipzig 1892.

F.H. Perrin, Whose Absorption Law? ***Opt. Soc. Am.*** 38 (1948) 72-74.

* * * * * * * *

Fig. 1 : Pierre Bouguer (1698 - 1758)

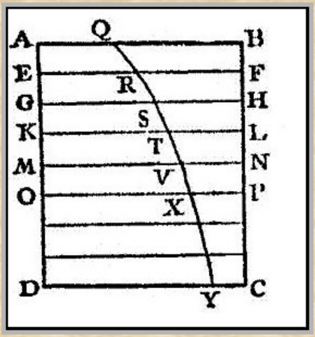

Fig. 2

The transmission of light in a transparent body ABCD. The length QB represents the incident intensity, RF the intensity after having traversed the first layer, SH the intensity after having traversed the second layer, etc. The ***x***-axis (axis of abscissae) is BC.

(From Bouguer, 1729)

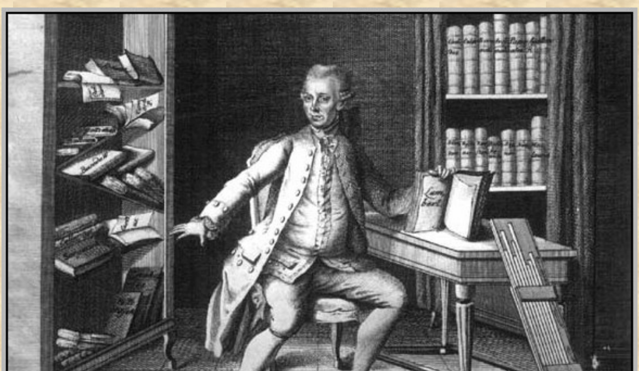

Fig. 3 : Johann Heinrich Lambert (1728 - 1777)

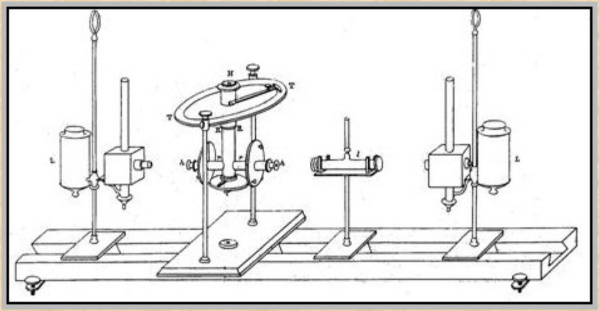

Fig. 4 :
Photometer devised by Beer. Light from the lamp at the right-hand side passes through an absorption cell, whereas the lamp at the left-hand side is a reference source. The photometer is adjusted so that the observed intensities from the two light sources are equal.

(From Beer, 1852)

Previous | Home Page | Next

MEMBERS' PAPER

High Accuracy Measurements of X-ray Mass Attenuation Coefficients

Christopher T. Chantler, Martin D. de Jonge,
Chanh Q. Tran, Zwi Barnea

School of Physics, University of Melbourne
Victoria 3010, Australia

We have applied the x-ray extended range technique (XERT) to measure mass attenuation coefficients up to two orders of magnitude more accurately than any previously reported in the literature. In this article we describe the application of the XERT to the investigation of systematic effects due to harmonic energy components in the x-ray beam, scattering and fluorescence from the absorbing sample, the bandwidth of the x-ray beam, and thickness variations across the absorber. The measurements are used for comparison with different calculations of mass attenuation coefficients, and to identify particular regions where these calculations fail. Absolutely scaled data with robust error estimates in the region of the x-ray absorption fine structure (XAFS) can be used to improve the accuracy of XAFS analysis and can provide a rigourous test of the absolute scale of XAFS modelling. Results of the technique can determine atomic and solid state properties, including bond radii, to high accuracy.

I. INTRODUCTION

The accuracy of x-ray optical constants can significantly affect the optimisation of an experimental arrangement and the interpretation of experimental results. For example, x-ray atomic form factors and mass attenuation coefficients can affect the interpretation of tomographic and crystallographic experiments, and can influence the design of x-ray refractive lenses and zoneplates. Despite significant differences between various tabulations of mass attenuation coefficients, these tabulations are often used with little discrimination.

Fig. 1 presents the mass attenuation coefficients of molybdenum appearing in the FFAST [1–3] and XCOM [4, 5] tabulations as raw values (top) and as a difference from the FFAST tabulated values (bottom). Significant differences between the calculated values are observed across a wide range of energies both above and below the absorption edge of molybdenum at about 20 keV, and exceed 15% at some energies. Similar discrepancies between calculated values appear to be present in all tabulations, for most elements, and across most x-ray energy ranges.

The results of measurements of the mass attenuation coefficients of molybdenum compiled by Hubbell et al. [6, 7] are plotted on ***Fig. 1***.

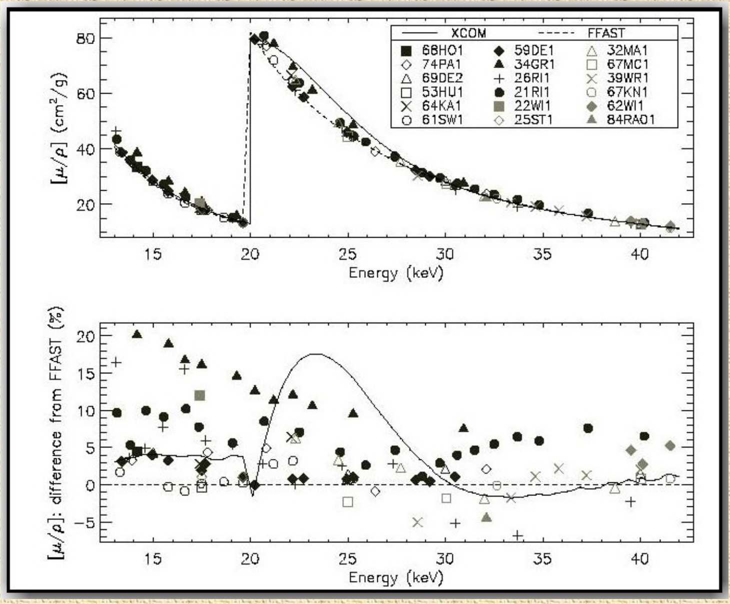

Figure 1

Top: The mass attenuation coefficient for molybdenum as given in the FFAST [1–3] and XCOM tabulations [4, 5], and as reported by a variety of previous experimental investigations (experimenter code referred to in the key is as per Hubbell et al. [6, 7]).

Bottom: Discrepancies between theoretical predictions and experimental measurements presented as a percentage difference from the FFAST tabulation. The difference between the FFAST and XCOM tabulations is greater than about 4% over most of the energy range shown here, but rises to over 15% over several keV above the absorption edge. Differences of 10%–20% between measured values whose typical claimed uncertainties are about 2% indicate the presence of unrecognized systematic errors affecting these measurements.

These experimental results generally claim uncertainties of between 1% and 3%. The spread of the measurements demonstrates that the measurement accuracy is much poorer than claimed. These measurements are unable to resolve differences between the FFAST and XCOM or other tabulations. Discrepancies between the results of independent investigations indicate that there are significant and undiagnosed systematic errors which have affected the accuracy of the measurements, particularly addressed in earlier years by Creagh et al.[8, 9]. This article describes our methods for investigating these particular sources of systematic error and their effects on the measured mass attenuation coefficients.

II. METHODOLOGY

We use the XERT and probe a number of dimensions of the measurement parameterspace to determine the influence of a range of systematic effects on the measured values [10]. We make measurements under optimum conditions and continue these measurements well beyond the optimum range as, for example, represented by the Nordfors criterion. Critical examination of the nature of the breakdown of the measurement is used to identify the cause of the measurement failure, and thus to estimate the implications, if any, on measurements made under optimal conditions. This article describes our treatment of systematic errors arising from the presence of harmonic energy components, the effects of secondary radiation (scattering and fluorescence), the influence of the finite x-ray energy bandwidth, and from absorber thickness variations. These methods have been applied to measurements of the mass attenuation coefficients of copper [11], silicon [12], silver [13], and molybdenum [15]. While such examples can be seen to be ideal test standards, other investigations in progress investigate tin, but also compounds such as ZnSe and to glass (SiO_2). The technique is quite general and can be applied to metals, crystals and glasses. Of course, synchrotron beamlines vary dramatically and therefore corresponding experimental techniques must be adapted accordingly. Again, the final accuracy attainable may be limited by specific systematics of the sample, of the beamline, or of the time allocated by the synchrotron for the particular experiment. Explicit tests for the effects of a wide range of systematic errors have enabled us to rigorously justify experimental accuracies of between 0.02%–0.7%.

Fig. 2 presents a schematic of the experimental setup that we have used to measure mass attenuation coefficients. The exact details of the experimental arrangement vary slightly in response to the operational details of the synchrotron beamline. We have used bending magnet, undulator, and elliptical multipole wiggler sources to produce a spectrum of high-brilliance x-rays. The x-ray beam is monochromated by double reflection from a monochromator, usually silicon, and preferably from planes [such as (111) or (311)] with a 'forbidden' second order reflection. The monochromator is usually detuned to reduce the passage of higher-order harmonics into the beam [16, 17].

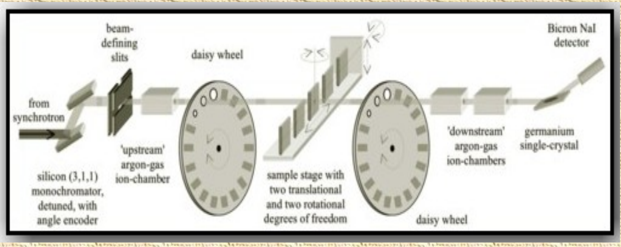
beam-defining slits
daisy wheel
Bicron NaI detector
from synchrotron
'upstream' argon-gas ion-chamber
silicon (3,1,1) monochromator, detuned, with angle encoder
sample stage with two translational and two rotational degrees of freedom
'downstream' argon-gas ion-chambers
germanium single-crystal
daisy wheel

Figure 2

Typical arrangement of the experimental components used to employ the XERT

Counting statistics have limited measurement precision in a number of reported measurements of mass attenuation coefficients [18–21]. We have used high-brilliance synchrotron sources to obtain measurements with high statistical precision. The improved statistical precision of our measurements has made it possible to detect a range of systematic effects which would otherwise not be discernible from the data.

The x-ray beam is collimated to a cross-section of approximately $1 \times 1 mm^2$ by the use of two orthogonal slits. An 'upstream' ion chamber is used to monitor the intensity of the incident beam, and a 'downstream' ion chamber to record the intensities of the attenuated and unattenuated beams. We use matched ion chambers, and optimize for strong positive correlations between the counts recorded in the upstream and downstream ion chambers [22, 23]. Accordingly, gas is flowed through the ion chambers in a serial configuration. We have generally recorded measurements with correlation coefficient R 0.99 between the upstream and downstream detectors, which enables us to determine the ratio of the measured intensities to high precision. A loss of correlation is a signature of poorly matched or optimised ion chambers, of excessive sample attenuation or electronic noise, or of other undiagnosed errors of the experimental technique. This precision enables us to detect the effects of systematic errors on the measurement with high sensitivity.

A number of specimens of widely differing attenuation ($0.1 \leq \left[\frac{\mu}{\rho}\right] [\rho t] \leq 10$) are used to measure the x-ray attenuation at each energy. Conventional literature in the past has investigated XAFS and related phenomena with only a single sample, and has attempted to follow the Nordfors criterion above and below the edge with the same sample. Creagh et al. [8, 9] noted that different thicknesses yield different magnitudes of systematics from particular sources. Hence a range of multiple thicknesses is generally needed for accurate determinations.

The samples are mounted on the sample stage, shown in ***Fig. 2,*** which is located mid-way between the upstream and the downstream ion chambers. The stage can be rotated about two axes and translated in two directions orthogonal to the beam. The samples are placed and replaced in the path of the beam to high precision by the use of a computer-controlled motorized driving system.

Daisy-wheels [24] are located between the sample stage and the ion chambers. These daisy-wheels have on their perimeters a series of apertures which are used to admit different amounts of secondary (fluorescent and scattered) photons into the ion chambers. In addition to these apertures, a large number of attenuating foils are mounted on the perimeter of the daisy-wheels and these can, like the apertures, be placed in the path of the beam by suitable rotation of the daisy-wheel. The thicknesses of the daisy-wheel foils are chosen to span an extremely large range of x-ray attenuations, typically with ($0.01 \leq \left[\frac{\mu}{\rho}\right] [\rho t] \leq 50$) at the nominal x-ray energy.

III. HARMONIC COMPONENTS

When attenuation measurements are made using a monochromatic x-ray beam, the logarithm of the intensity plotted as a function of the absorber thickness t falls on a straight line whose slope is the product of the mass attenuation coefficient $\left[\frac{\mu}{\rho}\right]$ and the density ρ of the foil material, as described by the Beer-Lambert relation

$$\ln\left(\frac{I}{I_0}\right) = -\left[\frac{\mu}{\rho}\right] rt \qquad (1)$$

where I and I_0 are the attenuated and unattenuated intensities respectively. The product $\left[\frac{\mu}{\rho}\right]\rho$ is sometimes referred to as the linear absorption coefficient ***μ,*** but we use the alternate notation for consistency.

In practice, $\ln(\boldsymbol{I} / \boldsymbol{I}_0)$ can be non-linear with thickness due to the presence of other spectral components in the beam. In particular, harmonic multiples of the fundamental x-ray energy may be present in the beam, especially when their intensities in the source spectrum are significant. While detuning of the monochromator crystal may suppress the propagation of these harmonic components in the beam, the residual effect on the measured attenuation may remain significant.

The relative efficiency of detection of the fundamental and of the harmonic x-rays influences the effect of any harmonic components on an attenuation experiment. For example, the ion-chamber detectors used in our work exhibit a rapid decrease in detection efficiency with increasing x-ray energy. However, the effective harmonic content, i.e., as perceived by the detector, can still be significant, as was the case in our measurement of the mass attenuation coefficient of silicon [12].

For a fraction $\boldsymbol{x}$ of harmonic x-rays (with attenuation coefficient $\left[\frac{\mu}{\rho}\right]_{\boldsymbol{h}}$) in the incident monochromatised beam (with $\left[\frac{\mu}{\rho}\right]_{\boldsymbol{f}}$ the attenuation coefficient for the fundamental energy), the measured attenuation of the x-ray beam $\left[\frac{\mu}{\rho}\right]_{\boldsymbol{meas}} \boldsymbol{\rho} t$ will be [24].

Fig. 3 shows the measured attenuation of eleven sets of aluminium foils (with thicknesses between 15 µm and 1 mm) in the path of an x-ray beam monochromated by a detuned, double-reflection silicon (111) channelcut monochromator set to select 5 keV x-rays. These foils were placed in the beam by suitable rotation of the daisy wheel. This technique is accurate, reproducible and rapid. This work was performed at the bending magnet beamline 20B of the Photon Factory synchrotron at Tsukuba.

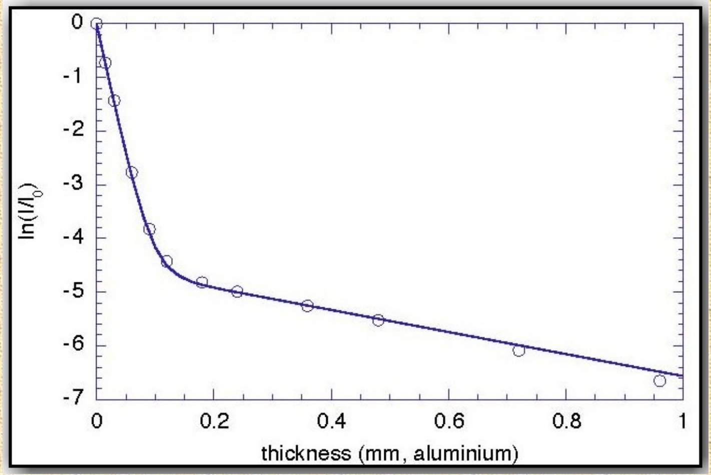

Figure 3

The attenuation $\ln(I/I_0)$ as a function of the thickness of aluminium absorber in the x-ray beam with a silicon monochromator set to 5 keV.
o = experimental values; solid line = curve of best fit corresponding to an admixture of (1.09 ± 0.02)% third-order harmonic (15 keV) following Equation (2)

$$-\left[\frac{\mu}{\rho}\right]_{meas} r\mathrm{t} = \ln\left(\frac{I}{I_0}\right)_{meas} = \ln\left[(1-x)\exp\left\{-\left[\frac{\mu}{\rho}\right]_f r\mathrm{t}\right\} + \exp\left\{-\left[\frac{\mu}{\rho}\right]_h r\mathrm{t}\right\}\right] \quad (2)$$

The experimental values follow a straight line until the thickness of aluminium increases to such an extent that the detected radiation consists overwhelmingly of the more energetic 15 keV third-order harmonic. When this occurs, one observes an inflection with the gradient approaching that of $\left[\frac{\mu}{\rho}\right]_\rho$ of aluminium at the energy of the third-order harmonic.

This inflection in the plot provides clear evidence for the presence of a third-order harmonic [the (222) second order reflection for silicon is 'forbidden']. The solid curve in ***Fig. 3*** is the calculated thickness dependence of the attenuation of aluminium for 5 keV x-rays with an admixture of (1.09 ± 0.02)% of the 15 keV third-order harmonic, as can be confirmed by extrapolating the second 'linear' portion of the graph back to zero thickness.

A minimum of three samples of accurately known thickness is required to simultaneously determine x, $\left[\frac{\mu}{\rho}\right]_f$ and $\left[\frac{\mu}{\rho}\right]_h$ If $\left[\frac{\mu}{\rho}\right]_h$ is provided by a separate experiment (or theory) then the use of three samples overdetermines the problem and allows for error analysis, or alternatively allows the possible observation of an additional harmonic component.

In ***Fig. 4*** we have determined the harmonic content of the beam at several energies by using three well-calibrated thicknesses of silicon. Attenuation measurements of the foils at the harmonic energy, yielding $\left[\frac{\mu}{\rho}\right]_h$, have been used to provide the gradient for the harmonic component dominating in the high-thickness portion of the graph. This figure shows clearly the effect of the harmonic components on the mass attenuation coefficient measured using the thickest sample at the lower energies. The harmonic component decreases rapidly as the fundamental energy increases due to the changing ion-chamber efficiencies and the lesser amounts of the harmonic x-rays in the synchrotron source spectrum. Our measurements of the effect of the beam harmonic component have enabled us to determine the mass attenuation coefficient of silicon at these low energies to accuracies of 0.3% – 0.5%.

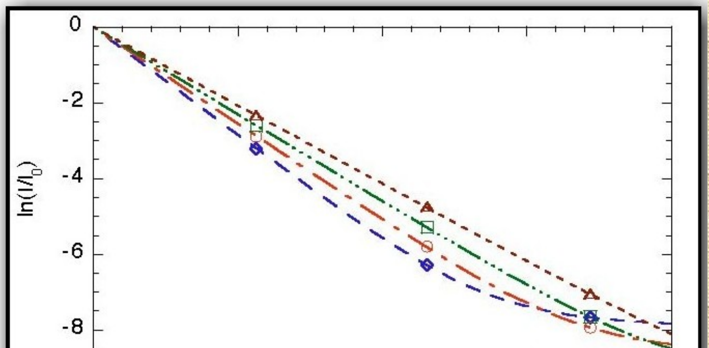

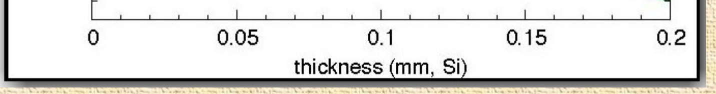

Figure 4

A harmonic component measurement with three well calibrated thicknesses provides a constant and reliable indicator of accuracy in attenuation measurements.
Measurements made at :
◊–5.0 keV, o–5.2 keV, □–5.4 keV, and Δ–5.6 keV.
Calculated curves for each energy pass through the measured values.

IV. SECONDARY RADIATION

The mass attenuation coefficient $\left[\frac{\mu}{\rho}\right]$ can be determined accurately using the setup depicted in ***Fig. 2*** provided the ion chambers only record the intensities of the attenuated and unattenuated beams. However, the dominant attenuating processes in the 1 keV - 100 keV energy range — photoelectric absorption and Rayleigh and Compton scattering — produce secondary x-rays which may also reach the detectors. Incident x-ray photons may be elastically or inelastically scattered by the absorbing material or by the air path. X-ray fluorescence resulting from photoelectric absorption can contribute significantly to the recorded count rate when measurements are made on the high-energy side of an absorption edge. The contribution of these effects depends on the x-ray optics and collimation, the angle subtended by the apertures at the sample, the photon energy, the detector response function and on the atomic number and thickness of the absorbing sample.

We have made measurements with apertures of various diameters placed between the absorbing specimen and the ion chambers. These apertures, mounted on the daisy wheels, admit various amounts of the secondary radiation into the detectors. The secondary radiation yields a systematic change in the measured mass attenuation coefficients correlating with the aperture diameter and the sample thickness, and also varying as a function of photon energy.

Fig. 5 shows the percentage discrepancy in the measured mass attenuation coefficients of silver, comparing those obtained with a large (16 mm diameter) and medium (8 mm diameter) aperture. This figure shows that the reading recorded using the large aperture is up to 0.2% less than that measured using the medium aperture. This effect is largest immediately above the silver absorption edge at about 25.2 keV, where the fluorescent yield is greatest and the incident beam is most attenuated.

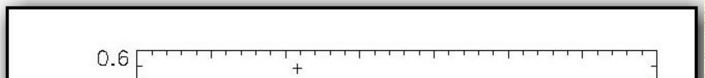

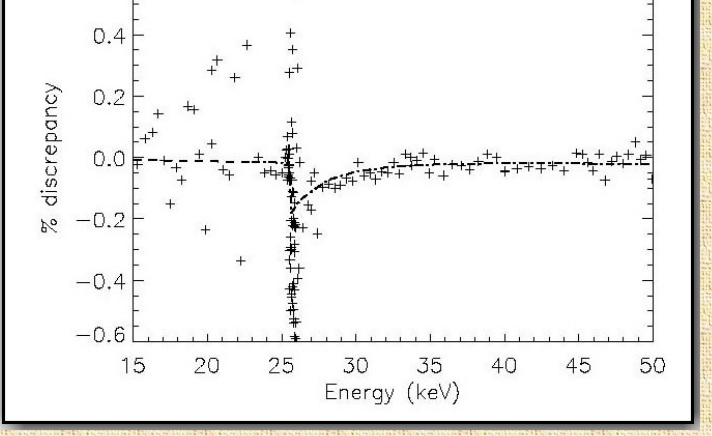

Figure 5

Percentage discrepancy between the mass attenuation coefficients of silver measured using the large and medium diameter apertures. The dashed and dash-dot lines show the prediction for the 10 µm and 100 µm foils used for the measurements.

We have modelled the effect of the dominant fluorescent and Rayleigh scattered x-rays on the measured mass attenuation coefficients [25]. Our model calculates the contribution to the counts recorded in the upstream and the downstream ion chambers resulting from fluorescent radiation emitted by the absorber and from Rayleigh scattering by the absorbing material and the air-path between the ion chambers. Self-absorption corrections are applied to all secondary photons. The prediction of this model is shown on ***Fig. 5***, and is in good agreement with the observed discrepancies. These investigations have been carried out in the course of determining the mass attenuation coefficients of silver accurate to 0.27%– 0.7%.[13].

V. X-RAY BANDWIDTH

Even the most highly monochromatic source produces a spectrum of x-rays of finite bandwidth. Typical bandwidths vary from $\frac{\Delta E}{E} \approx 10^{-5}$ to $\frac{\Delta E}{E} \approx 10^{-3}$ for x-rays monochromated by reflection from a crystal monochromator, or approximately 0.5 eV to 10 eV across the central x-ray energy range. The most obvious consequence of having a distribution of energies in the x-ray beam is that instead of measuring the mass attenuation coefficient corresponding to a single x-ray energy, we measure the combined attenuation at these energies weighted by the intensity of each x-ray energy component. Since each energy component will in general have a different attenuation coefficient, the original distribution of energies in the x-ray beam – the beam energy profile – will change gradually as the beam is attenuated by the foil, with the less attenuated components gradually increasing their relative intensity over the more attenuated components. This change in the beam energy profile will yield a nonlinearity of the measured mass attenuation coefficient as a function of foil thickness [26].

Away from absorption edges the mass attenuation coefficient varies sufficiently slowly for the bandwidth effect not to be detected. However, on the absorption edge the mass attenuation coefficient changes rapidly and the effect of the bandwidth is significant.

Fig. 6 presents the values obtained from measurements made along the molybdenum absorption edge. This work was performed on the 1-ID beamline at XOR sector 1 at the APS. The beam was produced by an undulator and was monochromated by reflection from the (3,1,1) planes of a pair of silicon crystals. The values presented in ***Fig. 6*** are in good agreement and could be used to report 'excellent' x-ray absorption near-edge structure (XANES).

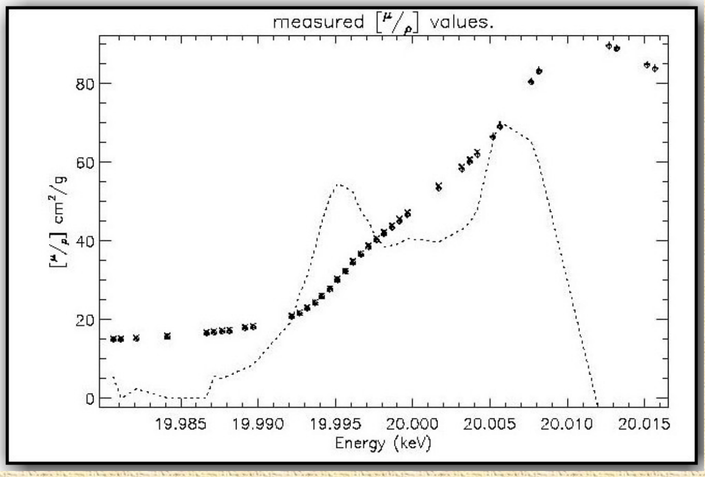

Figure 6

Values of the mass attenuation coefficient of molybdenum obtained from measurements in the near-edge region. At each energy measurements have been made with three thicknesses of foil, represented by three different symbols:
× — 100 µm; + — 50 µm; ◊— 25 µm.
The consistency of the experimental values is too good for the measurements at each energy to be clearly resolved on this scale. The gradient of the weighted mean of the measurements made at each energy is plotted as a dotted line, on a relative scale.

However, the discrepancies between the values obtained using foils of different thickness, which cannot easily be resolved in ***Fig. 6***, are presented in ***Fig. 7***, and in fact lead to beam-line dependencies in reported XANES studies [14].

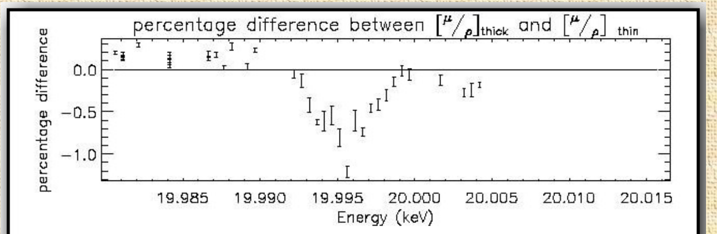

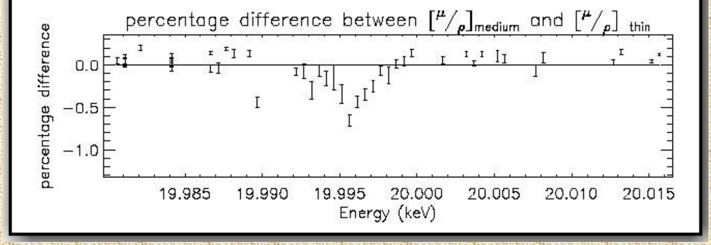

Figure 7

Percentage difference between the mass attenuation coefficients obtained using the thick (top) and medium (bottom) foils and that obtained using the thin foil. The prominent dip in the discrepancies occurring at about 19.995 keV coincides with the point where the gradient of the mass attenuation coefficient reaches its maximum value (c.f. ***Fig. 6***)

This figure presents the percentage difference between the mass attenuation coefficients determined using the thick (top figure) and medium (bottom figure) foils and that determined using the thinnest foil. There is a gradient correlated discrepancy between the measured values, the magnitude of the discrepancy increasing as the thickness of the foil used to make the measurement increases. The measured mass attenuation coefficient (subscript ***m***) is related to the beam energy profile and the 'true' mass attenuation coefficient (subscript ***t***) by [26]

$$\exp\left(-\left[\frac{\mu}{\rho}\right]_{m,E_0}[\rho t]\right) = \int_0^\infty \tilde{I}_{E_0}\exp\left(-\left[\frac{\mu}{\rho}\right]_{t,E}[\rho t]\right)dE \qquad (3)$$

where E_0 is the central energy of the beam profile and $\tilde{I}_0$ is the normalized incident beam energy profile, defined as

$$\tilde{I}_0 = \frac{I_0}{\int_0^\infty I_0\, dE} \qquad (4)$$

We have inverted ***Eq. (3)*** under the assumption of the approximate linearity of the mass attenuation coefficient on the scale of the beam bandwidth, and have determined the bandwidth of our x-ray beam to be 1.57 eV±0.03 eV at 20 keV [26]. We have also used the linearised approach to determine a correction to the mass attenuation coefficients measured on the absorption edge of molybdenum [15].

Fig. 8 presents the correction to the mass attenuation coefficients obtained along the absorption edge, and shows that the finite x-ray bandwidth has affected the measurements by up to 1.4%. The structure shown in ***Fig. 8*** is significant, and would be of particular interest in XAFS and XANES investigations.

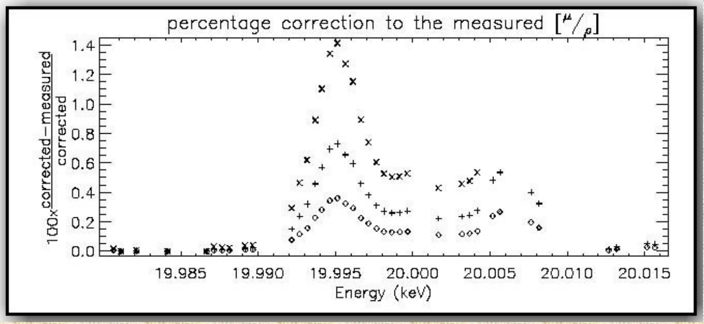

Figure 8

Percentage correction to the mass attenuation coefficients measured in the neighborhood of the absorption edge and in the region of the XAFS, evaluated using the linearized approximation.

VI. THE FULL-FOIL MAPPING TECHNIQUE

In a number of recent reports [18-20, 27-30] it has been observed that, for accuracies between 0.5%-2%, a dominant source of error in the measurement of mass attenuation coefficients is the accurate determination of the sample thickness along the actual path traversed by the x-ray beam. We have developed a full-foil mapping technique for determining the mass attenuation coefficient on an absolute scale which overcomes previous limitations due to uncertainties in the sample thickness.

Traditionally the local value of the integrated column density has been determined as the product of the density and the thickness. The local thickness was determined by a variety of techniques using micrometry [11, 12, 21, 30, 31], profilometry [11], optical microscopy [32], step-profilometry [33], and x-ray scanning techniques [11, 12, 21]. Measurements of sample thickness have an advantage in that they probe the variation of the thickness across the surface of the foil. However, each of the techniques mentioned above is subject to a range of fundamental limitations affecting precision and accuracy which are difficult to overcome [11, 12, 34], which represent a major limitation on the precision and accuracy of the determination of the mass attenuation coefficient.

More recent measurements have used the areal density of the absorber, which we term the integrated column density, for the determination of the mass attenuation coefficient [11, 12, 18-20, 27, 29, 35-37]. These measurements have generally been limited to accuracies of 0.5%- 2% due to variation in the thickness, which has limited the determination of the local integrated column density of the absorbing specimen along the column actually traversed by the beam.

The Beer-Lambert equation describes the attenuation of x-rays of a given energy passing through an absorber by

$$- \ln \left(\frac{I}{I_0}\right)_{xy} = \left[\frac{\mu}{\rho}\right][rt]_{xy} \tag{5}$$

where I and I_0 represent the attenuated and unattenuated beam intensities respectively, $\left[\frac{\mu}{\rho}\right]$ the mass attenuation coefficient of the absorbing material at a given energy, and $[rt]_{xy}$ the integrated column density along the path taken by the x-ray beam through the location (***x***, ***y***) on the absorber. It is obvious from ***Eq. (5)*** that measurements made at a single (***x, y***) location on an absorber cannot be used to determine the mass attenuation coefficient to a higher level of accuracy than that to which the integrated column density of the absorber at that point is known.

The mass attenuation coefficient of a foil absorber can be determined by measuring the attenuation at (***x, y***) locations to determine an attenuation profile $-\ln\left(\frac{I}{I_0}\right)_{xy}$ of the absorber. The mass attenuation coefficient can then be determined from the average of the measured attenuation profile since, for a homogenous sample with fixed $\left[\frac{\mu}{\rho}\right]$ [38] ,

$$\overline{-\ln\left(\frac{I}{I_0}\right)_{xy}} = \overline{\left[\frac{\mu}{\rho}\right][\rho t]_{xy}} = \overline{\left[\frac{\mu}{\rho}\right]}\;\overline{[\rho t]_{xy}} = \left[\frac{\mu}{\rho}\right]\frac{m}{A} \tag{6}$$

where the mass ***m*** of a given area ***A*** of the foil is used to determine the average integrated column density $\overline{[\rho t]}$. The mass and area of the foil can be measured to high accuracy using well-established techniques, for example by using an optical comparator to determine area and an accurate microgram balance to measure mass. In contrast with earlier techniques, XERT can determine the mass attenuation coefficient to high accuracy without directly determining the local integrated column density at any point of the absorber.

Figure 9 shows the attenuation profile of a nominally 254-µm-thick molybdenum foil. This attenuation profile has been determined from the attenuation measurements of the sample mounted in a plastic holder. To determine the attenuation profile of the absorbing sample alone we have subtracted the small fitted holder component from the measured attenuation profile.

Using this technique we have recently determined the mass attenuation coefficients of molybdenum to an accuracy of 0.028% [38] and of silver to accuracies in the range 0.27%–0.7% [34]. Measurements of the attenuation profile of the silver foils at different energies have confirmed the reproducibility of the measurement at this high accuracy.

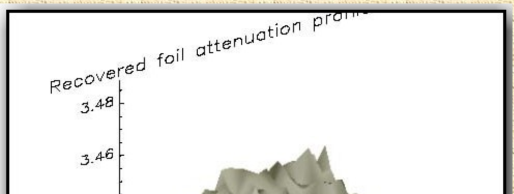

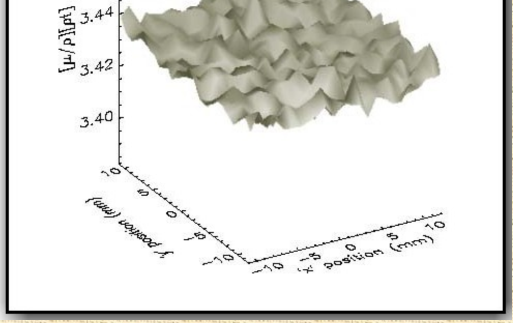

Figure 9

Attenuation profile of a molybdenum foil. The attenuation profile was produced from an x-ray scan of the foil mounted in a plastic holder. The small holder contribution was fitted and subtracted from these measurements. The x-ray beam used to make the measurements was 1×1 mm^2 and measurements were taken at 1 mm intervals across the foil.

VII. INFORMING THEORIES OF PHOTOABSORPTION

We have measured the mass attenuation coefficients of copper [11], silicon [12], silver [13], and molybdenum [15] using various synchrotron sources. Following the principles of the XERT, measurements were made over an extended range of the measurement parameter-space, and were investigated for evidence of systematic errors. We have developed a technique to determine an accurate value of the mass attenuation coefficient from raster measurements made across the surface of an absorber. We have also detected and corrected effects resulting from a small fraction of harmonic energy components in the synchrotron beam, from fluorescent radiation produced in an absorbing specimen, and from the finite bandwidth of the x-ray beam. By applying these techniques we have improved measurement accuracies by over one order of magnitude.

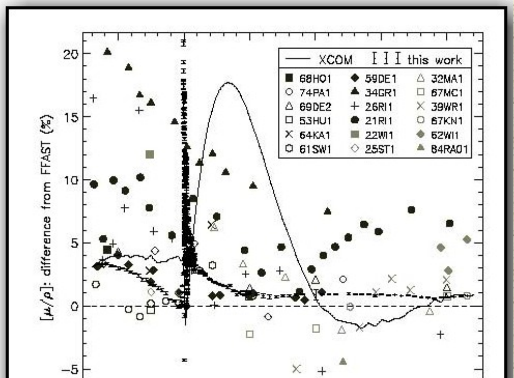

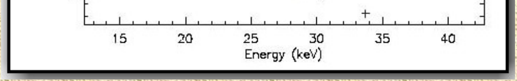

Figure 10

Our measured values of the mass attenuation coefficients of molybdenum as a percentage difference from the tabulated FFAST values [1–3]. Measurement uncertainties of 0.02%–0.15% are indicated by the error bars. The spike in the difference of our values from the FFAST tabulated values occurring near the absorption edge is due to the XANES, which is not modelled by either tabulation.
Also shown are the percentage differences between the tabulated XCOM [4, 5] values and the experimental values tabulated by Hubbell ***et al***. [6, 7], compared with FFAST.

Figure 10 presents our measured values for molybdenum compared with the FFAST tabulated values. Also shown are the XCOM calculated values and the experimental values tabulated in Hubbell et al. [6, 7], compared to the FFAST values. The trend of the percentage difference between our values and the FFAST tabulation is generally smooth to within the claimed measurement uncertainty, indicating that the uncertainties are appropriately estimated. By contrast, the point-to-point variations in the trend of individual experimental measurements tabulated by Hubbell ***et al.*** is typically no better than 1%–2% and is therefore the limiting possible precision of any of these measurements. The accuracy must necessarily be lower than this point-wise inconsistency. The larger inconsistencies between the different sets of measurements prove the magnitude of present systematic errors in those data sets. Our measurements are free from many such systematic errors because we have explicitly investigated our measurements for their presence and have proven that each has a small or negligible remaining signature in our results.

The XCOM tabulated values exhibit a large oscillation with respect to the FFAST values over the energy range from 20 keV to 30 keV or 40 keV. Oscillatory behavior in the calculated values has been observed elsewhere [1, 2] and may be the result of an incompletely converged calculation. Our measurements clearly show that the XCOM tabulation is in error in this region. Above about 40 keV the XCOM values are in good agreement with our measurements.

The FFAST tabulation estimates uncertainties – arising from calculational convergence precision and the limitations of various approximations –

at about 50% within $EK \lesssim E \lesssim 1.001E_K$,
10% -20% within $1.001E_K \lesssim E \lesssim 1.1E_K$,
3% within $1.1E_K \lesssim E \lesssim 1.2E_K$, and
1% for $E \gtrsim 1.2E_K$ (E_K is the K-shell absorption-edge energy).

These estimates are in accord with the differences of ***Fig. 10***. The difference between our measurements and the FFAST tabulation is stable at about 0.5%–1% at energies above 25 keV. Below the absorption edge the measurements exhibit a more complex pattern of discrepancy, but fall between the XCOM and FFAST values. Although this supports the accuracies of the FFAST tabulation, the higher accuracy of the experimental measurements also implies a possible systematic error of this magnitude in this atomic regime. The measured values are 1%–3% higher than the FFAST tabulated values within a range of about 5 keV above the absorption edge. Although this is within the FFAST uncertainty, a similar above-edge enhancement observed for copper [11] and silver [13] suggests that the FFAST values are systematically low in this region.

The presence of this discrepancy in measurements of three elements indicates new physics in the above-edge energy region [13, 15, 39, 40]. Further experiments are required to determine whether this discrepancy is present for other elements and above other (e.g.***L***-shell) absorption edges. Such measurements will provide further clues which will inform future calculations of the mass attenuation coefficients. XAFS structures are solved routinely and hundreds of publications appear per annum. Limitations in theoretical predictions and XAFS analytical frameworks lead to significant uncertainty in results, impairing structural predictions and preventing ab initio determination. Our accurate measurements and robust error estimates of the attenuation of molybdenum in the above-edge region have been used to improve the XAFS determinations by between 5% and 70% [41]. A deeper understanding of the interactions between x-rays and matter requires accurate measurements so that each contributing process may be compared with theoretical models. Relative measurements provide crucial information but absolute attenuation measurements provide additional demanding tests of theory and computation.

ACKNOWLEDGEMENTS

We acknowledge the assistance of the synchrotron staff at each of the beamline facilities involved in this work, being beamline 20B of the Photon Factory in Tsukuba, and beamlines 1-BM, 1-ID, and 12-BM of the APS. This work was supported by the Australian Synchrotron Research Program, which is funded by the Commonwealth of Australia under the Major National Research Facilities Program, and by a number of grants of the Australian Research Council. Use of the Advanced Photon Source was supported by the U.S. Department of Energy, Basic Energy Sciences, Office of Energy Research, under Contract No. W31109Eng38.

REFERENCES

[1] C. T. Chantler, "Detailed tabulation of atomic form factors, photoelectric absorption and scattering cross section, and mass attenuation coefficients in the vicinity of absorption edges in the soft x-ray (Z=30–36, Z = 60–89, E = 0.1 keV–10 keV), addressing convergence issues of earlier work," Journal of Physical and Chemical Reference Data 29, pp. 597–1056, 2000.

[2] C. T. Chantler, "Theoretical form factor, attenuation and scattering tabulation for Z=1–92 from E=1–10 eV to E=0.4–1.0 MeV," Journal of Physical and Chemical Ref-erence Data 24, pp. 71–85, 1995.

[3] C. T. Chantler, K. Olsen, R. A. Dragoset, A. R. Kishore, S. A. Kotochigova, and D. S. Zucker, X-Ray Form Factor, Attenuation and Scattering Tables (version 2.0). [Online] Available: http://physics.nist.gov/ffast National Institute of Standards and Technology, Gaithersburg, MD., 2003

[4] M.J. Berger, J. H. Hubbell, S. M. Seltzer, J. S. Coursey, and D. S. Zucker, XCOM: Photon Cross Section Database (version 1.2) [Online] Available: http://physics.nist.gov/xcom, National Institute of Standards and Technology, Gaithersburg, MD., 1999.

[5] M.J. Berger and J. H. Hubbell, "Photon cross sections on a personal computer," NIST Standard Reference Database 8 87, p. 3597, 2004.

[6] J. H. Hubbell, NISTIR 5437, National Institute of Standards and Technology, Gaithersburg, MD., 1994.

[7] J. H. Hubbell, J. S. Coursey, J. Hwang, and D. S. Zucker, Bibliography of photon total cross section (attenuation coefficient) measurements (version 2.3) [online] Available:http://physics.nist.gov/photoncs, National Institute of Standards and Technology, Gaithersburg, MD., 2003.

[8] D. C. Creagh and J. H. Hubbell, "Problems associated with the measurement of x-ray attenuation coefficients. I. Silicon. Report on the International Union of Crystallography X-ray Attenuation Project," Acta Crystallographica Sect. A 43, pp. 102–12, 1987.

[9] D. C. Creagh and J. H. Hubbell, "Problems associated with the measurement of x-ray attenuation coefficients. II. Carbon. Report on the International Union of Crystallography X-ray Attenuation Project," Acta Crystallographica Sect. A 46, pp.402–8, 1990.

[10] C. T. Chantler, C. Q. Tran, D. Paterson, D. J. Cookson, and Z. Barnea, "X-ray extended range technique for precision measurement of the x-ray mass attenuation coefficient and Im(f) for copper using synchrotron radiation," Physics Letters A 286, pp. 338–46, 2001.

[11] C. T. Chantler, C. Q. Tran, Z. Barnea, D. Paterson, D. J. Cookson, and D. X. Balaic, "Measurement of the x-ray mass attenuation coefficient of copper using 8.85– 20 keV synchrotron radiation," Physical Review A 64, 062506, 2001.

[12] C. Q. Tran, C. T. Chantler, Z. Barnea, D. Paterson, and D. J. Cookson, "Measurement of the x-ray mass attenuation coefficient and the imaginary part of the form factor of silicon using synchrotron radiation," Physical Review A 67, 042716, 2003.

[13] C. Q. Tran, C. T. Chantler, Z. Barnea, M. D. de Jonge, B. B. Dhal, C. T. Y. Chung, D. Paterson, and J. Wang, "Measurement of the x-ray mass attenuation coefficient of silver using the x-ray extended range technique," Journal of Physics B 38(1), pp. 89–107, 2005.

[14] J. L. Glover, C. T. Chantler, The Analysis of X-ray Absorption Fine Structure: Beamline independent interpretation, Phys. Lett. A submitted (2006)

[15] M. D. de Jonge, C. Q. Tran, C. T. Chantler, Z. Barnea, B. B. Dhal, D. J. Cookson, W.K. Lee, and A. Mashayekhi, "Measurement of the x-ray mass attenuation coefficient and determination of the imaginary component of the atomic form factor of molybdenum over the 13.5–41.5 kev energy range," Physical Review A 71(3), 032702, 2005.

[16] J. H. Beaumont and M. Hart, "Multiple Bragg reflection monochromators for synchrotron x-radiation," Journal of Physics E 7, pp. 823–9, 1974.

[17] U. Bonse, G. Materlik, and W. J. Schroder, "Perfect crystal monochromators for synchrotron x-radiation," J. Appl. Crystallogr. 9, pp. 223–30, 1976.

[18] R. Nathuram, I. S. S. Rao, and M. K. Mehta, "Photoelectric cross sections for 6–20 kev photons in beryllium, carbon, magnesium, aluminum, silicon, copper, silver, and lead," Physical Review A 37,pp. 4978–81, 1988.

[19] F. Machali, G. G. Al Barakati, A. A. El Sayed, and W. J. Altaf, "The photoelectric cross section of gamma rays in the energy range 43 to 152 keV," Journal of Physics F 17, pp. 1279–84, 1987.

[20] L. Gerward, "X-ray attenuation coefficients of carbon in the energy range 5 to 20 keV," Acta Crystallographica Sect. A 39, pp. 322–5, 1983.

[21] J. F. Mika, L. J. Martin, and Z. Barnea, "X-ray attenuation of silicon in the energy range 25–50 keV," Journal of Physics C 18, pp. 5215–23, 1985.

[22] C. T. Chantler, C. Q. Tran, D. Paterson, Z. Barnea, and D. J. Cookson, "Monitoring fluctuations at a synchrotron beamline using matched ion chambers. I. Modelling, data collection and deduction of simple measures of association," X-Ray Spectrometry 29(6), pp. 449–58, 2000.

[23] C. T. Chantler, C. Q. Tran, D. Paterson, D. J. Cookson, and Z. Barnea, "Monitoring fluctuations at a synchrotron beamline using matched ion chambers. II. Isolation of component noise sources, and application to attenuation measurements showing increased precision by two orders of magnitude," X-Ray Spectrometry 29(6), pp. 459–66, 2000.

[24] C. Q. Tran, Z. Barnea, M. D. de Jonge, B. B. Dhal,D. Paterson, D. J. Cookson, and C. T. Chantler, "Quantitative determination of major systematics in synchrotron x-ray experiments: seeing through harmonic components," X-Ray Spectrometry 32, pp. 69–74, 2003.

[25] C.Q. Tran, M. D. de Jonge, Z. Barnea, and C. T. Chantler, "Absolute determination of the effect of scattering and fluorescence on x-ray attenuation measurements," Journal of Physics B 37, pp. 3163–3176, 2004.

[26] M.D. de Jonge, Z. Barnea, C. Q. Tran, and C. T. Chantler, "X-ray bandwidth: determination by on edge absorption and effect on various absorption experiments," Physical Review A 69, 022717, 2004.

[27] W. Dachun, D. Xunliang, W. Xinfu, Y. Hua, Z. Hongyu, S. Xinyin, and Z. Guanghua, "X-ray attenuation coefficients and photoelectric cross sections of Cu and Fe in the range 3 keV to 29 keV," Nucl. Instrum. and Meth. in Phys. Res. Sect. B: Beam Interactions with Materials and Atoms 71, pp. 241–8, 1992.

[28] D. K. S. Reddy, K. Premachand, V. R. K. Murty, J. R. Rao, and V. Lakshminarayana, "Photoelectric interaction below the K edge," Physical Review A 13, pp. 326–9, 1976.

[29] L. Unonius and P. Suortti, "Mass attenuation coefficients of the elements Ti, V, Fe, Co, Ni, Cu and Zn for the K-emission lines between 4.51 and 10.98 keV," J. Appl. Crystallogr. 22, pp. 46–52, 1989.

[30] L.Gerward, "X-ray attenuation coefficients and atomic photoelectric absorption cross sections of silicon," Journal of Physics B 14, pp. 3389–95, 1981.

[31] J.L. Lawrence, "X-ray attenuation coefficients of graphite in the range 0.40 to 1.54 °A," Acta Crystallographica Sect. A 35, pp. 316–8, 1979.

[32] J. Balthazar Rodrigues and C. Cusatis, "Determination of x-ray photoelectric absorption of Ge and Si avoiding solid state effects," Nucl. Instrum. and Meth. in Phys. Res. Sect. B: Beam Interactions with Materials and Atoms 179, pp. 325–33, 2001. , "Mass absorption coefficient of tungsten for 1600–2100 eV," Physical Review B 65, 064111, 2002.

[33] Z. H. Levine, S. Grantham, and I. McNultyM. D. de Jonge, Z. Barnea, and C. Q. Tran, "Analysis of x-ray absorption fine structure using absolute x-ray mass attenuation coefficients: application to molybdenum," Radiation Physics and Chemistry 75, pp. 1559-1563, 2006

[34] C.Q. Tran, Z. Barnea, C. T. Chantler, and M. D. de Jonge, "Accurate determination of the thickness or mass per unit area of thin foils and single crystal wafers for x-ray attenuation measurements," Review of Scientific Instruments 75(9), 2004.

[35] M. Angelone, T. Bubba, and A. Esposito, "Measurement of the mass attenuation coefficient for elemental materials in the range $6 \le Z \le 82$ using x-rays from 13 up to 50 keV," Applied Radiation and Isotopes 55(4), pp. 505– 11, 2001.

[36] L. Gerward, "X-ray attenuation coefficients of beryllium in the energy range 5 to 20 keV," Acta Crystallographica Sect. A 45, pp. 1-3, 1989.

[37] R. S. Prakhya, K. Parthasaradhi, V. Lakshminarayana, K. L. Narasimham, K. V. Ramanaiah, and S. B. Reddy, "Measurement of K--shell photoelectric cross sections by the indirect method," Physical Review A 33, pp. 2440-3, 1986.

[38] M. D.de Jonge, Z. Barnea, C. T. Chantler, and C. Q. Tran, "Full-foil x-ray mapping of integrated column density applied to the absolute determination of mass attenuation coefficients," Measurement Science and Technology 15, pp. 1811-1822, 2004.

[39] D. C. Creagh, "The use of the form factor formalism in crystallography," Nucl. Instrum. and Meth. in Phys. Res. Sect. A: Accelerators, Spectrometers, Detectors and Associated Equipment 280, pp. 180-8, 1989.

[40] D. C. Creagh, The Chinese Journal of Physics 29(4), pp. 299-325, 1991. "Atomic form factor, the dispersion corrections and their role in x-ray crystallography,"

[41] L. F. Smale, C. T. Chantler,

[42] Y. Joly, "X-ray absorption near edge structure calculations beyond the muffin-tin approximation," Physical Review B 63, 125120, 2001.

[43] E. C. Cosgriff, C. T. Chantler, C. Witte, L. Smale, and C. Q. Tran, "Atomic cluster structure calculations of the X-ray near-edge absorption of silver," Physics Letters A 343, pp. 174-80, 2005.

[44] C. Witte, C. T. and Chantler, E. C. Cosgriff, and C. Q. Tran, "Atomic cluster calculation of the X-ray near-edge absorption of copper", Radiation Physics and Chemistry 75, pp. 1582-1585, 2006.

[45] M.D. de Jonge, "High-accuracy measurements of the mass attenuation coefficients of molybdenum and tin: testing theories of photoabsorption," Ph.D. thesis, 2005.

==============================

Previous | Home Page

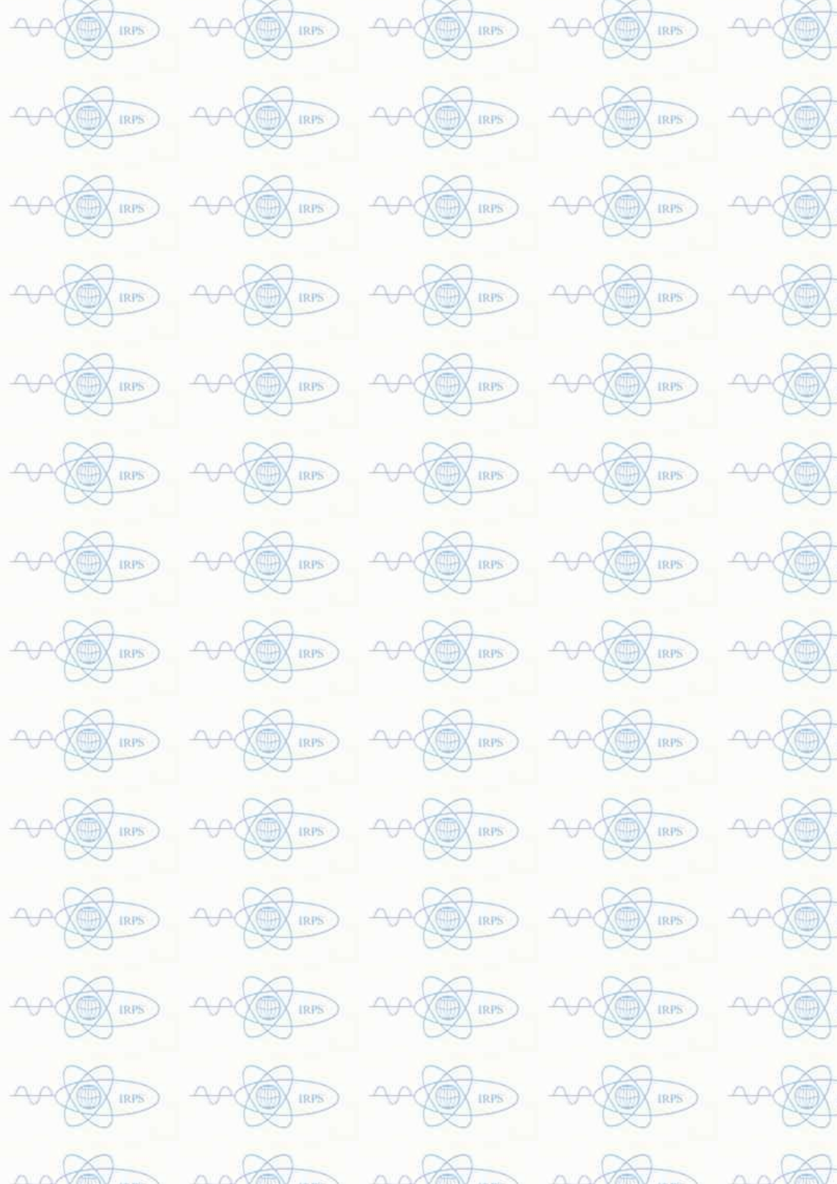

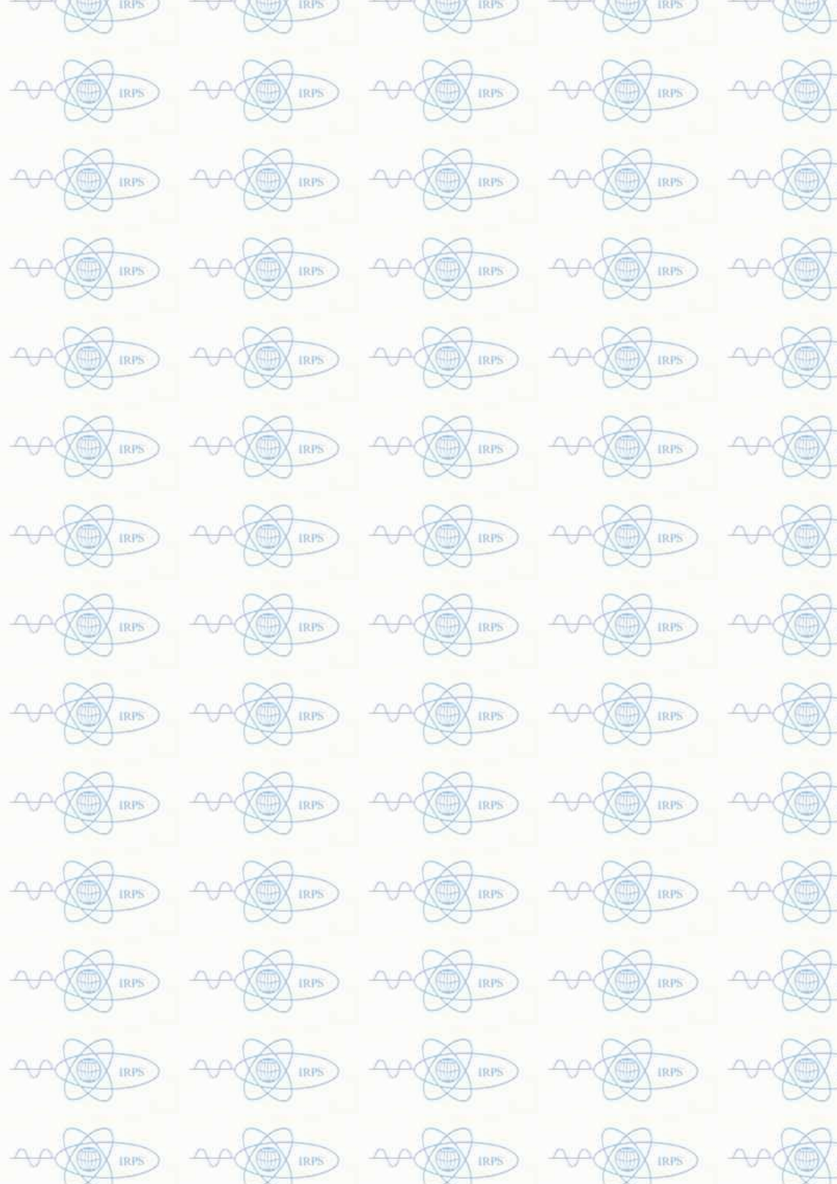
IRPS

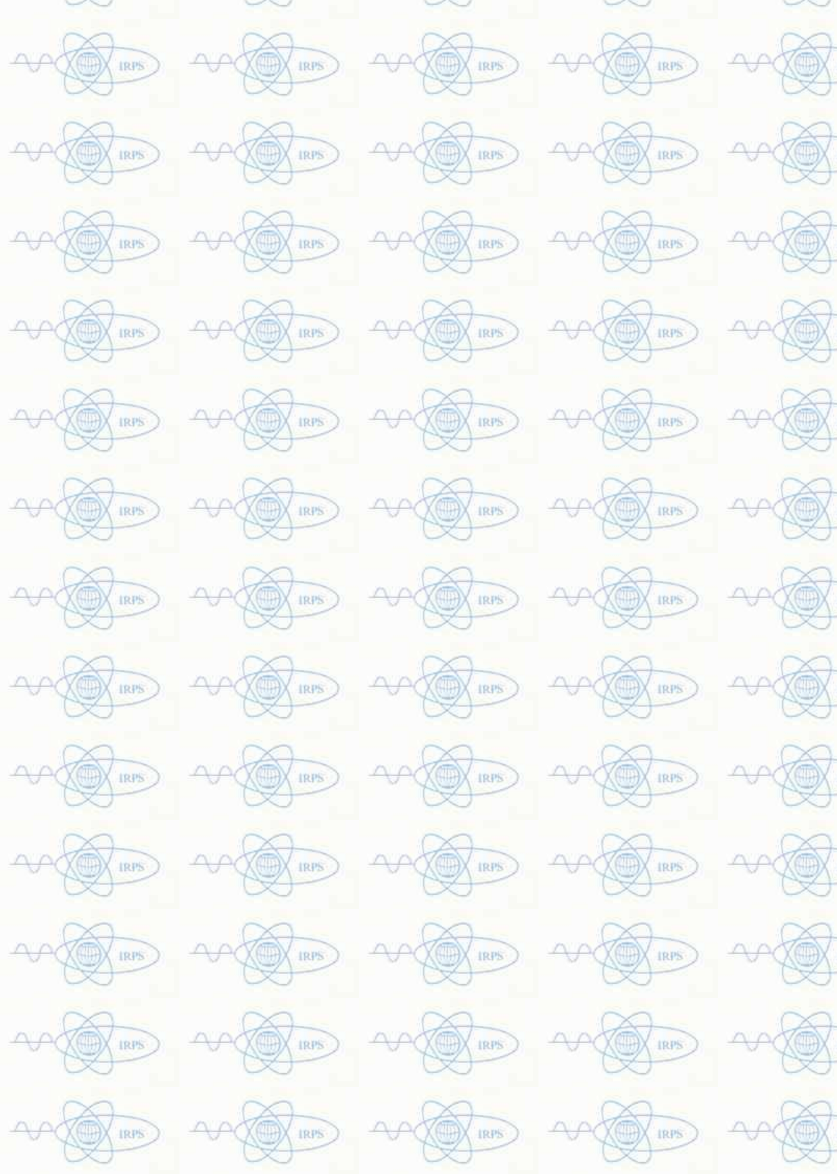

IRPS

IRPS IRPS IRPS IRPS
IRPS IRPS IRPS IRPS
IRPS IRPS IRPS IRPS
IRPS IRPS IRPS IRPS
IRPS IRPS IRPS IRPS
IRPS IRPS IRPS IRPS
IRPS IRPS IRPS IRPS
IRPS IRPS IRPS IRPS
IRPS IRPS IRPS IRPS
IRPS IRPS IRPS IRPS
IRPS IRPS IRPS IRPS
IRPS IRPS IRPS IRPS
IRPS IRPS IRPS IRPS
IRPS IRPS IRPS IRPS

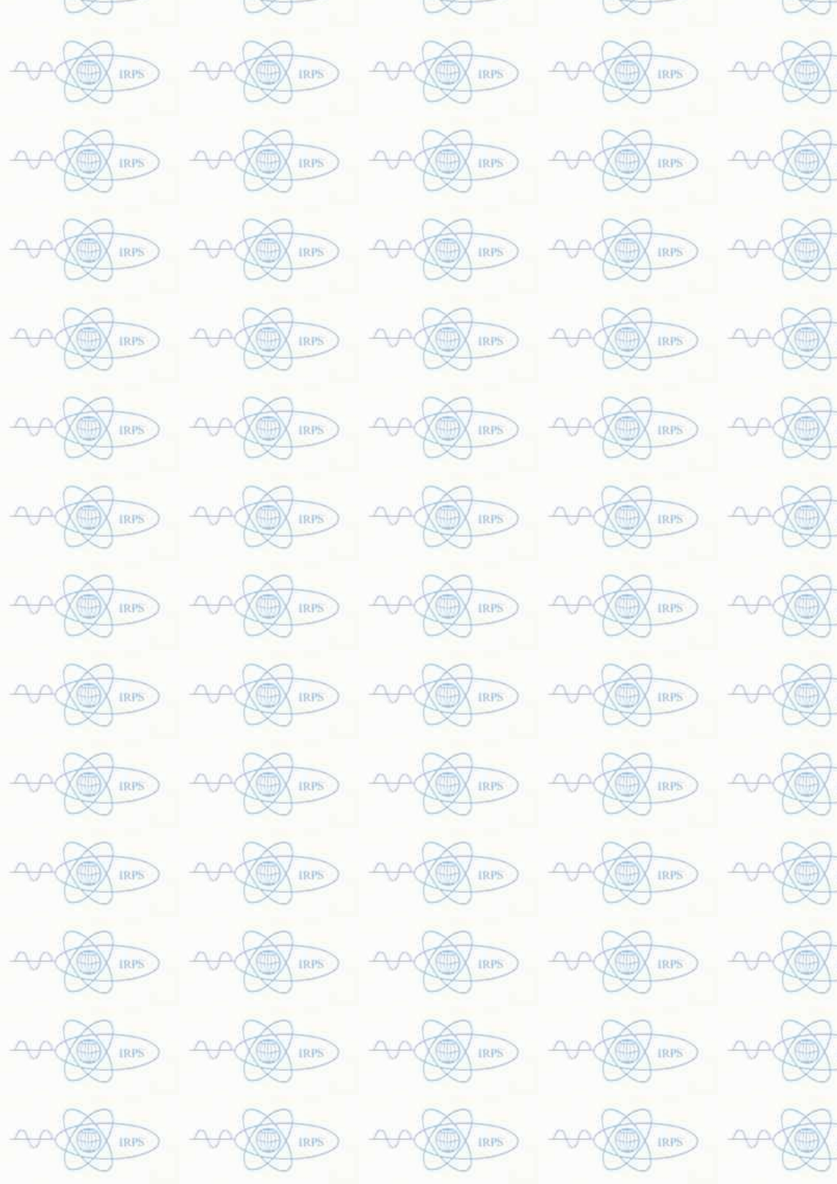

IRPS